

---

# Meta-learning Feature Representations for Adaptive Gaussian Processes via Implicit Differentiation

---

**Wenlin Chen**

University of Cambridge  
MPI for Intelligent Systems  
wc337@cam.ac.uk

**Austin Tripp**

University of Cambridge  
ajt212@cam.ac.uk

**José Miguel Hernández-Lobato**

University of Cambridge  
jmh233@cam.ac.uk

## Abstract

We propose Adaptive Deep Kernel Fitting (ADKF), a general framework for learning deep kernels by interpolating between meta-learning and conventional learning. Our approach employs a bilevel optimization objective where we meta-learn feature representations that are generally useful across tasks, in the sense that task-specific Gaussian process models estimated on top of such features achieve the lowest possible predictive loss on average across tasks. We solve the resulting nested optimization problem using the implicit function theorem. We show that ADKF contains Deep Kernel Learning and Deep Kernel Transfer as special cases. Although ADKF is a completely general method, we argue that it is especially well-suited for drug discovery problems and demonstrate that it significantly outperforms previous state-of-the-art methods on a variety of real-world few-shot molecular property prediction tasks and out-of-domain molecular optimization tasks.

## 1 Introduction

A wide range of real-world applications, particularly problems in healthcare, require machine learning algorithms to make robust predictions with well-calibrated uncertainty given a small training set. Taking drug discovery as an example where the goal is to find novel molecules which optimally fulfill various metrics, Bayesian optimization (BO) is potentially useful for accelerating and automating this process, wherein data collection is guided by an acquisition function. BO is highly sensitive to the quality of the predictions and uncertainty estimates provided by the surrogate model used [9]. Although neural networks have been successfully applied to solving molecular property prediction problems [13], they are notoriously non-robust and overconfident, especially when trained on small datasets. With a small number of available measurements at the early stage of a drug discovery project, it is extremely difficult to fit a neural network with good predictive performance, let alone good predictive uncertainty.

Meta-learning improves the predictive performance of neural networks in the low-data regime by leveraging a large number of small datasets, so that knowledge can be transferred among related low-data tasks. FS-Mol [40] is a recently proposed dataset for benchmarking few-shot learning in drug discovery, which contains thousands of molecular property prediction tasks and defines a robust evaluation procedure. Surprisingly, many popular meta-learning and self-supervised pretraining methods cannot even beat Random Forest on these tasks. The best performing baseline method in FS-Mol, namely ProtoNet [38], employs a neural network to meta-learn data representations which are then fed into a nearest centroid classifier. Although ProtoNet ranks first among FS-Mol baseline methods, its nearest centroid classifier is unsatisfactory in many aspects: 1) it lacks flexibility and tends to underfit when a large number of labeled examples are available; 2) it does not have a clear extension to solving regression problems; and 3) it provides no predictive uncertainty. One way to address these limitations is to replace the nearest centroid classifier with a Gaussian process (GP)

model [36]. This allows us to exploit the complementary strengths and weaknesses of neural networks and GPs for meta-learning, i.e., to combine the representation learning ability of neural networks and the robustness and uncertainty-awareness of GPs.

A popular way to combine neural networks and GPs is *deep kernel learning* [15, 52], wherein a kernel is constructed by first embedding data into a low-dimensional feature representation space using a neural network, then applying a “base kernel” (e.g., a Matérn kernel) to these feature representations. However, there is not a consensus on how to train these models on small datasets. Although early results suggested that the parameters of both neural network and base kernel could be tuned by maximizing the GP marginal likelihood (the conventional way of training GPs in the single-task setting) [52], subsequent work has shown that this can often lead to overfitting and a collapse in the GP’s uncertainty estimates [29]. This problem is especially acute with small datasets. Other researchers have proposed that the parameters in both parts can be jointly trained in a meta-learning framework to avoid overfitting [31, 44]. These works do not report overfitting, but they assume that all datasets can be well-approximated using exactly the same hyperparameters for the base kernel on each dataset. This assumption is unlikely to hold in practice: for example, different tasks may have different amounts of observation noise. Ultimately, neither of these strategies is a totally satisfactory way of training deep kernel GPs to transfer knowledge among small datasets.

In this work, we propose *Adaptive Deep Kernel Fitting* (ADKF) as a novel framework to address the aforementioned limitations when fitting deep kernel GPs to small datasets. ADKF *interpolates* between the conventional learning approach of [52] and the meta-learning approach of [31], which is done by partitioning the parameters of a deep kernel into two disjoint sets, then training one set with meta-learning and the other with conventional learning. This allows us to meta-learn generally useful feature representations across tasks, such that task-specific GP models estimated on top achieve the lowest possible predictive error on average across tasks. Although this creates a challenging nested optimization problem, we show that it can be solved using the implicit function theorem. We also demonstrate that ADKF contains [52] and [31] as special cases. While ADKF is a completely general method, we expect it to be especially well-suited for drug discovery problems, as will be argued in Section 3.3. We evaluate ADKF on a variety of real-world few-shot molecular property prediction tasks and out-of-domain molecular optimization tasks, showing that it significantly outperforms previous state-of-the-art methods.

## 2 Background

### 2.1 Gaussian Processes

Gaussian processes are tools for specifying priors over functions which are “sufficiently smooth”. A  $\mathcal{GP}(m_\theta(\cdot), c_\theta(\cdot, \cdot))$  is fully specified by a mean function  $m_\theta(\cdot)$  and a symmetric positive-definite covariance function  $c_\theta(\cdot, \cdot)$ . It is easy to perform principled model selection and obtain robust probabilistic predictions with GPs. Specifically, with a zero mean function<sup>1</sup> and a Gaussian likelihood with variance  $\sigma^2$ , the GP hyperparameters  $\theta$ <sup>2</sup> are chosen to maximize the log marginal likelihood on the training data  $(\mathbf{X}, \mathbf{y})$ , which trades off data fit and model complexity:

$$\log p(\mathbf{y} \mid \mathbf{X}, \theta) = -\frac{1}{2} \mathbf{y}^T (c_\theta(\mathbf{X}, \mathbf{X}) + \sigma^2 \mathbf{I}_N)^{-1} \mathbf{y} - \frac{1}{2} \log \det (c_\theta(\mathbf{X}, \mathbf{X}) + \sigma^2 \mathbf{I}_N) - \frac{N}{2} \log(2\pi).$$

By Bayes’ rule, the posterior predictive distribution  $p(\mathbf{y}_* \mid \mathbf{X}_*, \mathbf{X}, \mathbf{y}, \theta)$  on the test data  $(\mathbf{X}_*, \mathbf{y}_*)$  is a multivariate Gaussian with mean and variance shown below:

$$\mathbb{E}[\mathbf{y}_* \mid \mathbf{X}_*, \mathbf{X}, \mathbf{y}, \theta] = c_\theta(\mathbf{X}_*, \mathbf{X}) (c_\theta(\mathbf{X}, \mathbf{X}) + \sigma^2 \mathbf{I}_N)^{-1} \mathbf{y},$$

$$\text{Var}[\mathbf{y}_* \mid \mathbf{X}_*, \mathbf{X}, \mathbf{y}, \theta] = c_\theta(\mathbf{X}_*, \mathbf{X}_*) + \sigma^2 \mathbf{I}_{N_*} - c_\theta(\mathbf{X}_*, \mathbf{X}) (c_\theta(\mathbf{X}, \mathbf{X}) + \sigma^2 \mathbf{I}_N)^{-1} c_\theta(\mathbf{X}, \mathbf{X}_*).$$

### 2.2 Deep Kernel Learning

Deep kernel learning is a popular way to combine neural networks and GPs. A deep kernel is constructed by using the feature representations  $\mathbf{z} = \mathbf{f}_\phi(\mathbf{x})$  and  $\mathbf{z}' = \mathbf{f}_\phi(\mathbf{x}')$  as the inputs to a

<sup>1</sup>Following the convention [28, 36], we use zero mean functions for GP priors throughout the paper.

<sup>2</sup>We slightly abuse the notation and denote all trainable GP hyperparameters by  $\theta \in \Theta$ , including but not limited to kernel parameters and likelihood parameters.

base kernel  $c_\theta(\mathbf{z}, \mathbf{z}')$ , where  $\mathbf{f}_\phi : \mathcal{X} \rightarrow \mathbb{R}^n$  is a neural network feature extractor with learnable parameters  $\phi \in \Phi$ . The resulting deep kernel function  $k_{\theta, \phi}(\mathbf{x}, \mathbf{x}') = c_\theta(\mathbf{f}_\phi(\mathbf{x}), \mathbf{f}_\phi(\mathbf{x}'))$  can be used as covariance functions to specify deep kernel GP priors  $p(f) = \mathcal{GP}(f; 0, k_{\theta, \phi}(\cdot, \cdot))$ .

### 2.3 Few-shot Learning and Meta-learning

Few-shot learning is a type of learning problem that requires learning algorithms to be able to adapt to unseen tasks quickly given a few labeled examples. This typically requires knowledge transfer among related low-data tasks, as single-task learning algorithms would easily overfit.

Specifically, we are given a set of training tasks  $\mathcal{D} = \{\mathcal{T}_t\}_{t=1}^T$  and some unseen test tasks  $\mathcal{D}_* = \{\mathcal{T}_*\}$ . The uniform distribution over the training tasks in  $\mathcal{D}$  is denoted by  $p(\mathcal{T})$ . Each task  $\mathcal{T} = \{\mathcal{S}_\mathcal{T}, \mathcal{Q}_\mathcal{T}\}$  consists of a support set  $\mathcal{S}_\mathcal{T} = \{(\mathbf{x}_n, y_n)\}_{n=1}^{N_{\mathcal{S}_\mathcal{T}}}$  and a query set  $\mathcal{Q}_\mathcal{T} = \{(\mathbf{x}_m, y_m)\}_{m=1}^{N_{\mathcal{Q}_\mathcal{T}}}$ . The input data  $\mathbf{x}$  belongs to the input domain  $\mathcal{X}$  (e.g., molecule space), and the target variable  $y$  is either a continuous variable (e.g., inhibitory concentration) or a discrete variable (e.g., binary compound activity). We denote the collections of all input data points and all targets in the support set  $\mathcal{S}_\mathcal{T}$  by  $\mathcal{S}_\mathcal{T}^x$  and  $\mathcal{S}_\mathcal{T}^y$ , respectively.  $\mathcal{Q}_\mathcal{T}^x$  and  $\mathcal{Q}_\mathcal{T}^y$  are similarly defined for the query set  $\mathcal{Q}_\mathcal{T}$ . In a typical few-shot learning setting, a large number  $T = |\mathcal{D}|$  of training tasks are available, each of which has only a small number  $N_{\mathcal{S}_\mathcal{T}}$  of labeled examples in its support set  $\mathcal{S}_\mathcal{T}$ . The goal is to *meta-learn* a model on the training tasks  $\mathcal{D}$ , such that it can be quickly adapted to any unseen test task  $\mathcal{T}_*$ , i.e., to perform well on the query set  $\mathcal{Q}_{\mathcal{T}_*}$  given a small support set  $\mathcal{S}_{\mathcal{T}_*}$  associated with  $\mathcal{T}_*$  for test time adaptation.

## 3 Proposed Method: Adaptive Deep Kernel Fitting (ADKF)

This section describes the details of our proposed approach, Adaptive Deep Kernel Fitting (ADKF). At its core, ADKF is a method for fitting a GP with a deep kernel function  $k_{\theta, \phi}(\mathbf{x}, \mathbf{x}')$  (as defined in Section 2.2) using a combination of meta-learning and conventional deep kernel learning. Let  $\Psi = \Theta \cup \Phi$  represent the set of all parameters in a deep kernel. ADKF requires that  $\Psi$  be partitioned into two disjoint sets  $\Psi_{\text{meta}} \cup \Psi_{\text{adapt}} = \Psi$ , where  $\psi_{\text{meta}} \in \Psi_{\text{meta}}$  will be fit to a collection of tasks using meta-learning, and  $\psi_{\text{adapt}} \in \Psi_{\text{adapt}}$  will be adapted separately for each task.

### 3.1 General Framework

ADKF is most easily understood by separately considering  $\psi_{\text{meta}}$  and  $\psi_{\text{adapt}}$ . For a given task  $\mathcal{T}$  and meta-learned parameters  $\psi_{\text{meta}}$ , the task-specific parameters  $\psi_{\text{adapt}}$  are chosen to minimize the *training loss*  $\mathcal{L}_T$  evaluated on the task’s support set  $\mathcal{S}_\mathcal{T}$ , see (2) below. That is,  $\psi_{\text{adapt}}$  is *adapted* to the support set  $\mathcal{S}_\mathcal{T}$  of the task  $\mathcal{T}$  under consideration during both meta-training and meta-testing. The resulting optimal value for  $\psi_{\text{adapt}}$  given  $\psi_{\text{meta}}$  and  $\mathcal{S}_\mathcal{T}$  is called the *best response function*, denoted by  $\psi_{\text{adapt}}^*(\psi_{\text{meta}}, \mathcal{S}_\mathcal{T})$ . Knowing that  $\psi_{\text{adapt}}$  will be adapted separately to each task  $\mathcal{T}$ , the remaining problem is to choose a value for  $\psi_{\text{meta}}$  during meta-training. We propose to do this by minimizing the average *predictive validation loss*  $\mathcal{L}_V$  evaluated on the query set  $\mathcal{Q}_\mathcal{T}$  of a randomly sampled training task  $\mathcal{T} \sim p(\mathcal{T})$  given the optimal task-specific parameters  $\psi_{\text{adapt}}^*(\psi_{\text{meta}}, \mathcal{S}_\mathcal{T})$ , see (1) below. That is,  $\psi_{\text{meta}}$  is chosen such that our GP achieves the lowest possible average predictive loss on the query set  $\mathcal{Q}_\mathcal{T}$  of a randomly sampled training task  $\mathcal{T} \sim p(\mathcal{T})$  after  $\psi_{\text{adapt}}$  is adapted to the support set  $\mathcal{S}_\mathcal{T}$ . These objectives can be viewed jointly as forming the following *bilevel optimization* problem:

$$\psi_{\text{meta}}^* = \arg \min_{\psi_{\text{meta}}} \mathbb{E}_{p(\mathcal{T})} [\mathcal{L}_V(\psi_{\text{meta}}, \psi_{\text{adapt}}^*(\psi_{\text{meta}}, \mathcal{S}_\mathcal{T}), \mathcal{T})], \quad (1)$$

$$\text{s.t. } \psi_{\text{adapt}}^*(\psi_{\text{meta}}, \mathcal{S}_\mathcal{T}) = \arg \min_{\psi_{\text{adapt}}} \mathcal{L}_T(\psi_{\text{meta}}, \psi_{\text{adapt}}, \mathcal{S}_\mathcal{T}). \quad (2)$$

This formulates a meta-learning objective where we optimize the average predictive performance on the query sets (in Equation (1)) after processing the associated support sets (in Equation (2)).

We propose to solve this bilevel optimization problem using gradient-based optimization techniques. For the inner loop optimization problem (2), the gradient of  $\mathcal{L}_T$  w.r.t.  $\psi_{\text{adapt}}$  can be easily obtained by auto-differentiation. Therefore, for a given task  $\mathcal{T}$  and current meta-learned parameters  $\psi_{\text{meta}}$ , we can obtain  $\psi_{\text{adapt}}^*(\psi_{\text{meta}}, \mathcal{S}_\mathcal{T})$  using, e.g., the L-BFGS optimizer [23]. However, for the outer loop optimization problem (1), it is less straightforward how to compute the gradient of  $\mathcal{L}_V$  w.r.t.  $\psi_{\text{meta}}$ . This is because  $\psi_{\text{adapt}}^*(\psi_{\text{meta}}, \mathcal{S}_\mathcal{T})$  is a function of  $\psi_{\text{meta}}$  for a given task  $\mathcal{T}$ , making the expected

---

**Algorithm 1** Exact gradient computation for  $\psi_{\text{meta}}$  in Adaptive Deep Kernel Fitting (ADKF).

---

- 1: **Input:** a training task  $\mathcal{T}'$  and the current meta-learned parameters  $\psi'_{\text{meta}}$ .
- 2: Solve Equation (2) to obtain  $\psi'_{\text{adapt}} = \psi^*_{\text{adapt}}(\psi'_{\text{meta}}, \mathcal{S}_{\mathcal{T}'})$  using, e.g., the L-BFGS optimizer.
- 3: Compute  $\mathbf{g}_1 = \frac{\partial \mathcal{L}_V(\psi_{\text{meta}}, \psi_{\text{adapt}}, \mathcal{T}')}{\partial \psi_{\text{meta}}} \Big|_{\psi'_{\text{meta}}, \psi'_{\text{adapt}}}$  and  $\mathbf{g}_2 = \frac{\partial \mathcal{L}_V(\psi_{\text{meta}}, \psi_{\text{adapt}}, \mathcal{T}')}{\partial \psi_{\text{adapt}}} \Big|_{\psi'_{\text{meta}}, \psi'_{\text{adapt}}}$  by auto-diff.
- 4: Compute the Hessian  $\mathbf{H} = \frac{\partial^2 \mathcal{L}_T(\psi_{\text{meta}}, \psi_{\text{adapt}}, \mathcal{S}_{\mathcal{T}'})}{\partial \psi_{\text{adapt}} \partial \psi_{\text{adapt}}^T} \Big|_{\psi'_{\text{meta}}, \psi'_{\text{adapt}}}$  by auto-diff.
- 5: Solve the linear system  $\mathbf{v} \mathbf{H} = \mathbf{g}_2$  for  $\mathbf{v}$ .
- 6: Compute the mixed partial derivatives  $\mathbf{P} = \frac{\partial^2 \mathcal{L}_T(\psi_{\text{meta}}, \psi_{\text{adapt}}, \mathcal{S}_{\mathcal{T}'})}{\partial \psi_{\text{adapt}} \partial \psi_{\text{meta}}^T} \Big|_{\psi'_{\text{meta}}, \psi'_{\text{adapt}}}$  by auto-diff.
- 7: **Output:** the total derivative  $\frac{d \mathcal{L}_V}{d \psi_{\text{meta}}} = \mathbf{g}_1 - \mathbf{v} \mathbf{P}$ . ▷ Equations (3) and (4)

---

validation loss an *implicit function* of  $\psi_{\text{meta}}$  alone. Assuming that we have done the inner loop optimization and obtained  $\psi^*_{\text{adapt}}(\psi_{\text{meta}}, \mathcal{S}_{\mathcal{T}})$ , in order to update the meta-learned parameters  $\psi_{\text{meta}}$ , we need to compute the *total derivative* of the validation loss  $\mathcal{L}_V$  w.r.t.  $\psi_{\text{meta}}$  for any given task  $\mathcal{T}$ :

$$\frac{d \mathcal{L}_V}{d \psi_{\text{meta}}} = \frac{\partial \mathcal{L}_V}{\partial \psi_{\text{meta}}} + \frac{\partial \mathcal{L}_V}{\partial \psi^*_{\text{adapt}}} \frac{\partial \psi^*_{\text{adapt}}}{\partial \psi_{\text{meta}}}. \quad (3)$$

In Equation (3),  $\partial \mathcal{L}_V / \partial \psi_{\text{meta}}$  and  $\partial \mathcal{L}_V / \partial \psi^*_{\text{adapt}}$  can be easily obtained by auto-differentiation. However, the computation of the derivative of the best response function  $\partial \psi^*_{\text{adapt}} / \partial \psi_{\text{meta}}$  is more challenging, since  $\psi^*_{\text{adapt}}(\psi_{\text{meta}}, \mathcal{S}_{\mathcal{T}})$  is defined by an arg min function. Fortunately, Cauchy's *Implicit Function Theorem* (IFT) suggests a way of computing this quantity at the current meta-learned parameters  $\psi'_{\text{meta}}$  for a given task  $\mathcal{T}'$ :

$$\frac{\partial \psi^*_{\text{adapt}}}{\partial \psi_{\text{meta}}} \Big|_{\psi'_{\text{meta}}} = - \left( \frac{\partial^2 \mathcal{L}_T(\psi_{\text{meta}}, \psi_{\text{adapt}}, \mathcal{S}_{\mathcal{T}'})}{\partial \psi_{\text{adapt}} \partial \psi_{\text{adapt}}^T} \right)^{-1} \frac{\partial^2 \mathcal{L}_T(\psi_{\text{meta}}, \psi_{\text{adapt}}, \mathcal{S}_{\mathcal{T}'})}{\partial \psi_{\text{adapt}} \partial \psi_{\text{meta}}^T} \Big|_{\psi'_{\text{meta}}, \psi'_{\text{adapt}}}, \quad (4)$$

where  $\psi'_{\text{adapt}} = \psi^*_{\text{adapt}}(\psi'_{\text{meta}}, \mathcal{S}_{\mathcal{T}'})$ . A full statement of the IFT in the context of ADKF can be found in Appendix A. The only potential problem with Equation (4) is the computation and inversion of the Hessian matrix for  $\mathcal{L}_T(\psi_{\text{meta}}, \psi_{\text{adapt}}, \mathcal{S}_{\mathcal{T}'})$  w.r.t.  $\psi_{\text{adapt}}$ . This computation can be done exactly if  $\dim(\psi_{\text{adapt}})$  is small, otherwise an approximation to the inverse Hessian (e.g., [24, 4]) can be used. Combining (3) and (4), we have a recipe for computing the gradient  $d \mathcal{L}_V / d \psi_{\text{meta}}$  for a single task, as summarized in Algorithm 1. The expected gradient over  $p(\mathcal{T})$  is approximated by averaging the gradients for a batch of  $K$  randomly sampled training tasks. The meta-learned parameters  $\psi_{\text{meta}}$  can then be updated with the averaged gradient using, e.g., the Adam optimizer [19]. This procedure is repeated until convergence. In practice, we evaluate the performance of our model on a small set of validation tasks during meta-training, and use early stopping [33] to avoid overfitting of  $\psi_{\text{meta}}$ .

At meta-test time, we make predictions for each unseen test task  $\mathcal{T}_*$  based on the GP posterior predictive distribution with optimal parameters  $\psi^*_{\text{meta}}$  and  $\psi^*_{\text{adapt}}(\psi^*_{\text{meta}}, \mathcal{S}_{\mathcal{T}_*})$ :

$$p(\mathcal{Q}_{\mathcal{T}_*}^y \mid \mathcal{Q}_{\mathcal{T}_*}^x, \mathcal{S}_{\mathcal{T}_*}, \psi^*_{\text{meta}}, \psi^*_{\text{adapt}}(\psi^*_{\text{meta}}, \mathcal{S}_{\mathcal{T}_*})). \quad (5)$$

### 3.2 Specific Implementation

In section 3.1, the unspecified parts of the framework were the exact forms of the task-level loss functions  $\mathcal{L}_T$  and  $\mathcal{L}_V$ , and the partition of  $\Psi$ . Here we give details for the case where a Gaussian likelihood with variance  $\sigma^2$  is used, but this could be easily extended to approximate GPs with non-conjugate likelihoods (e.g., [50] for Bernoulli likelihood). We propose to use the negative log marginal likelihood evaluated on the support set  $\mathcal{S}_{\mathcal{T}}$  as the training loss  $\mathcal{L}_T$ , as is common practice:

$$\mathcal{L}_T(\psi_{\text{meta}}, \psi_{\text{adapt}}, \mathcal{S}_{\mathcal{T}}) = \frac{1}{2} \langle \mathcal{S}_{\mathcal{T}}^y, \mathbf{K}_{\mathcal{S}_{\mathcal{T}}}^{-1} \mathcal{S}_{\mathcal{T}}^y \rangle + \frac{1}{2} \log \det(\mathbf{K}_{\mathcal{S}_{\mathcal{T}}}) + \frac{N_{\mathcal{S}_{\mathcal{T}}}}{2} \log(2\pi), \quad (6)$$

where  $\mathbf{K}_{\mathcal{S}_{\mathcal{T}}} = k_{\psi_{\text{meta}}, \psi_{\text{adapt}}}(\mathcal{S}_{\mathcal{T}}^x, \mathcal{S}_{\mathcal{T}}^x) + \sigma^2 \mathbf{I}_{N_{\mathcal{S}_{\mathcal{T}}}}$ . We choose the predictive validation loss  $\mathcal{L}_V$  to be the negative log posterior predictive likelihood evaluated on the query set  $\mathcal{Q}_{\mathcal{T}}$  given the support set

$\mathcal{S}_T$ , also due to its common usage for making predictions with GPs:

$$\mathcal{L}_V(\psi_{\text{meta}}, \psi_{\text{adapt}}, \mathcal{T}) = -\log \mathcal{N}(\mathcal{Q}_T^y; \mathbf{K}_{\mathcal{Q}_T \mathcal{S}_T} \mathbf{K}_{\mathcal{S}_T}^{-1} \mathcal{S}_T^y, \mathbf{K}_{\mathcal{Q}_T} - \mathbf{K}_{\mathcal{Q}_T \mathcal{S}_T} \mathbf{K}_{\mathcal{S}_T}^{-1} \mathbf{K}_{\mathcal{S}_T \mathcal{Q}_T}), \quad (7)$$

where  $\mathbf{K}_{\mathcal{Q}_T} = k_{\psi_{\text{meta}}, \psi_{\text{adapt}}}(\mathcal{Q}_T^x, \mathcal{Q}_T^x) + \sigma^2 \mathbf{I}_{N_{\mathcal{Q}_T}}$  and  $\mathbf{K}_{\mathcal{S}_T \mathcal{Q}_T} = \mathbf{K}_{\mathcal{S}_T \mathcal{S}_T}^T = k_{\psi_{\text{meta}}, \psi_{\text{adapt}}}(\mathcal{S}_T^x, \mathcal{Q}_T^x)$ . This has the advantage that the prediction procedure during meta-testing (in Equation (5)) exactly matches the meta-training procedure, thereby closely following the principle of *learning to learn*. As for the partition of  $\Psi$ , it can be done in many ways in general. We propose to set  $\Psi_{\text{adapt}} = \Theta$  and  $\Psi_{\text{meta}} = \Phi$ , i.e., to meta-learn the feature extractor parameters  $\phi$  across tasks and to adapt the GP hyperparameters  $\theta$  for each individual task. The reasons for this are as follows: 1) it has a clear and intuitive interpretation: we are meta-learning a generally useful feature extractor  $\mathbf{f}_\phi$  such that it is possible on average to fit a low-loss GP to the feature representations extracted by  $\mathbf{f}_\phi$  for each individual task; 2) since  $\dim(\theta) < 10^2$  for essentially all common GP kernels, the Hessian in Equation (4) can be computed and “inverted” exactly during meta-training using Algorithm 1; 3) optimizing  $\psi_{\text{adapt}}$  in Equation (2) is computationally efficient, as it does not require backpropagating through the feature extractor  $\mathbf{f}_\phi$ ; 4) we conjecture that adapting the GP hyperparameters is more appropriate given the expected differences between tasks: two related tasks are more likely to have different noise levels or variances than to require substantially different feature representations.

### 3.3 Applications

While ADKF could be applied to any type of few-shot learning problem with a meta-dataset, we expect it to be especially well-suited for drug property prediction problems for the following reasons: 1) a large collection of drug property prediction tasks are available for meta-training (which share underlying physical mechanisms); 2) such tasks contain support sets of size  $\sim 10^2$ , which is both large enough to adapt the GP hyperparameters without overfitting and small enough so that exact GP inference is tractable; 3) significant training of the feature extractor is required, as there are no pretrained generally useful feature extractors for molecules available<sup>3</sup>; 4) domain expertise in drug discovery can be injected into the base kernel with hand-curated features and kernel combinations.

## 4 Related Work

**Learning with Deep Kernels.** ADKF is a *unified framework* containing Deep Kernel Learning (DKL) [52] and Deep Kernel Transfer (DKT) [31] as two special (extreme) cases. DKL is a single-task method without meta-learned parameters (i.e.,  $\Psi_{\text{meta}} = \emptyset$  and  $\Psi_{\text{adapt}} = \Psi$ ), where a separate deep kernel GP is learned for each task. DKT is a meta-learning method without task-specific parameters (i.e.,  $\Psi_{\text{meta}} = \Psi$  and  $\Psi_{\text{adapt}} = \emptyset$ ), where a common deep kernel GP is shared across tasks. Adaptive Deep Kernel Learning (ADKL) [44] is a meta-learning approach outside of our framework, wherein task-specific adaptation is amortized by a meta-learned task encoder: the input (i.e., data embedding) to the base kernel is conditioned on the embedding of the corresponding task’s support set.

**Meta-learning.** Meta-learning together with self-supervised pretraining has achieved great performance for few-shot learning problems in computer vision [20, 45, 47, 16, 30, 43, 2]. Some of the representative ideas for meta-learning are: MAML [8] meta-learns a common initialization of the model parameters as the starting point for task-specific parameter adaptation. ProtoNet [38] meta-learns a metric space for the nearest centroid classifier on top. CNP [11] constructs a conditional stochastic process, which is conditioned on the support sets via a meta-learned set encoder.

**Implicit Differentiation.** The IFT has been widely used in machine learning, such as solving minimax optimization problems [48], tuning hyperparameters [1, 25, 32, 24, 4], and meta-learning [34, 22, 3]. One challenge of applying IFT is the computation of the inverse Hessian. While early work computed this explicitly [21, 1], recent work employed various approximation techniques such as Neumann approximation [24, 4], conjugate gradient [32, 34, 3, 48], and the identity matrix [25].

<sup>3</sup>There are a few reasons for this: the total number of available measurements derived from wet-lab experiments is not comparable to the size of ImageNet [7]; unlike natural images, drug molecules lack meaningful invariances and local/global structures, and are not a clear manifold of the whole molecule space.

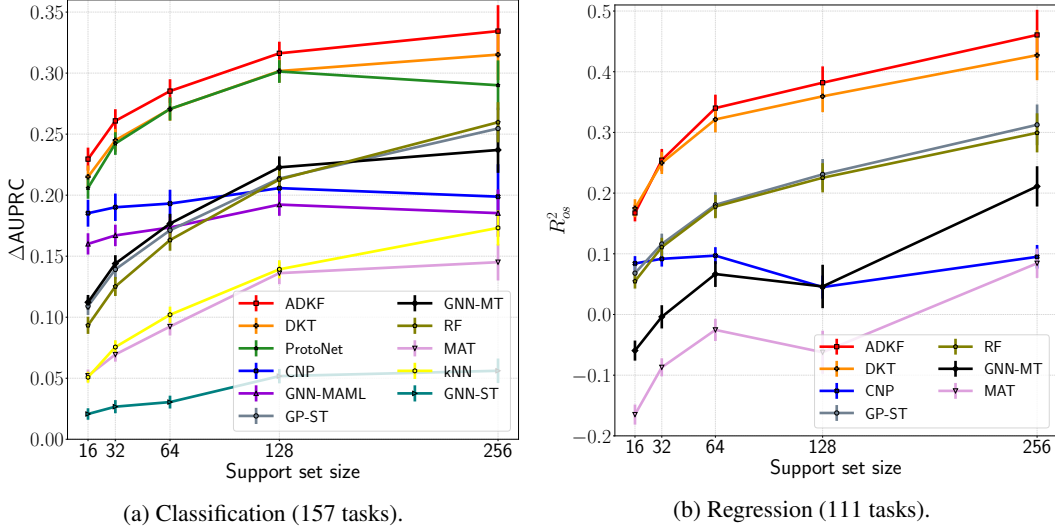


Figure 1: Mean performance with standard errors of all compared methods on all FS-Mol test tasks.

## 5 Experiments

This section aims to empirically demonstrate that the feature representations learned by ADKF are highly adaptive and generally useful. As argued in Section 3.3, our method is expected to be especially well-suited for problems in drug discovery. Because of this, we evaluate ADKF on the FS-Mol benchmark [40] (Section 5.1) and demonstrate that the feature representations learned by ADKF are transferable to out-of-domain molecular optimization tasks (Section 5.2).

We compare **ADKF** with four categories of learning algorithms: single-task methods, multi-task pretraining, self-supervised pretraining, and meta-learning methods. Representative methods are chosen within each category: Random Forest (**RF**), k-Nearest Neighbors (**kNN**), GP with Tanimoto kernel (**GP-ST**) [35], single-task GNN (**GNN-ST**) [13], multi-task GNN (**GNN-MT**) [6, 13], Molecule Attention Transformer (**MAT**) [26], Prototypical Network with Mahalanobis distance (**ProtoNet**) [38], Model-Agnostic Meta-Learning (**GNN-MAML**) [8], Conditional Neural Process (**CNP**) [11], and Deep Kernel Transfer (**DKT**) [31]. The implementations of RF, kNN, GNN-ST, GNN-MT, MAT, ProtoNet, and GNN-MAML are taken from [40]. The feature extractor architecture  $f_\phi$  used for CNP, DKT, and ADKF is the same as that used for ProtoNet in [40] (with the size of the feature representation being tuned on FS-Mol validation tasks). We use Matérn52 without automatic relevance determination (ARD) [28] as the base kernel in DKT and ADKF, since the typical support set sizes in few-shot learning are too small to adjust a relatively large number of ARD lengthscales. For ADKF, the lengthscale is initialized using the median heuristic [12] with a log-normal prior centered at the initialization. Detailed configurations of these methods can be found in Appendix B.

### 5.1 Few-shot Molecular Property Prediction

**Benchmark.** We conduct our evaluation on the FS-Mol benchmark [40], which is a carefully constructed set of few-shot learning tasks for molecular property prediction. FS-Mol contains over 5,000 tasks with 233,786 unique compounds from ChEMBL27 [27], split into training (4,938 tasks), validation (40 tasks), and test (157 tasks) sets. Each task is associated with a protein target. The original benchmark only considers binary classification of active/inactive compounds, since regressing the actual numeric activity target (IC50 or EC50) is known to be extremely difficult due to, e.g., large measurement noise. We nevertheless include regression (for the log numeric activity target) in our evaluation, as it is a desired and more preferred task to do in real-world drug discovery projects. All multi-task and meta-learning methods are trained from scratch on FS-Mol training tasks. MAT is pretrained on 2 millions molecules sampled from the ZINC15 dataset [41]. Following [31], we treat binary classification as  $\pm 1$  label regression in GP-ST, DKT, and ADKF. The classification results for RF, kNN, GNN-ST, GNN-MT, MAT, ProtoNet, and GNN-MAML are taken from [40].

Table 1: Mean ranks of all compared methods in terms of their performance on all FS-Mol test tasks.

(a) Classification (157 tasks).

Method	Support set size				
	16	32	64	128	256
GNN-ST	9.59	9.81	10.02	10.16	10.49
KNN	9.17	8.89	8.75	8.75	8.23
MAT	8.81	8.89	8.73	8.43	8.49
RF	6.88	6.74	6.21	5.68	4.42
GNN-MT	6.36	6.27	6.28	6.00	6.21
GP-ST	5.79	5.75	5.67	5.64	5.09
GNN-MAML	5.72	6.20	6.64	7.12	8.23
CNP	4.49	5.20	5.71	6.25	7.02
ProtoNet	3.72	3.21	3.00	2.88	3.76
DKT	3.22	3.04	2.91	2.91	2.67
ADKF	<b>2.25</b>	<b>2.00</b>	<b>2.07</b>	<b>2.18</b>	<b>1.38</b>

(b) Regression (111 tasks).

Method	Support set size				
	16	32	64	128	256
MAT	6.60	6.54	6.48	6.38	6.51
GNN-MT	5.72	5.67	5.51	5.50	5.23
RF	4.38	4.11	3.94	3.55	3.53
GP-ST	3.70	3.77	3.66	3.32	3.07
CNP	3.54	4.09	4.55	5.27	5.86
DKT	2.05	2.01	2.22	2.27	2.43
ADKF	<b>2.01</b>	<b>1.82</b>	<b>1.64</b>	<b>1.72</b>	<b>1.36</b>

Table 2:  $p$ -values from the two-sided Wilcoxon signed-rank test for statistical comparisons between ADKF and DKT. The null hypothesis is that the median of their performance differences on all FS-Mol test tasks is zero. The significance level is set to  $\alpha = 0.05$ .

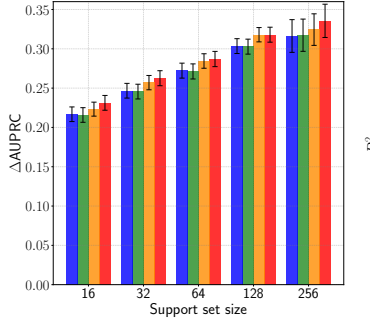
FS-Mol learning task	Support set size				
	16	32	64	128	256
Classification (157 tasks)	$1.4 \times 10^{-12}$	$8.1 \times 10^{-14}$	$2.3 \times 10^{-12}$	$1.0 \times 10^{-8}$	$3.4 \times 10^{-14}$
Regression (111 tasks)	$8.2 \times 10^{-2}$	$9.6 \times 10^{-2}$	$3.7 \times 10^{-5}$	$7.1 \times 10^{-5}$	$9.8 \times 10^{-7}$

**Evaluation Procedure.** The task-level metrics for binary classification and regression are  $\Delta\text{AUPRC}$  (change in area under the precision-recall curve) and  $R_{os}^2$  (out-of-sample coefficient of determination), respectively. Formulas for computing these metrics can be found in Appendix D. We follow exactly the same evaluation procedure as that in [40], where the averaged performance over ten different stratified support/query random splits of every test task is reported for each compared method. This evaluation process is performed for five different support set sizes 16, 32, 64, 128, and 256.

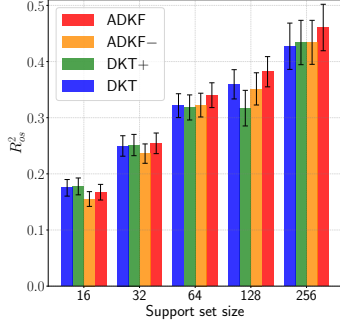
**Overall Performance.** Figure 1 shows the overall test performance of all compared methods. Note that RF is considered a strong baseline method, since it is widely used in real-world drug discovery projects and has comparable performance to multi-task and self-supervised pretraining methods. The results indicate that ADKF outperforms all the other compared methods at all considered support set sizes for the classification task. For the regression task, the performance gains of ADKF over the second best method, namely DKT, get larger as the support set size increases. In Table 1, we show that ADKF achieves the best mean rank for both classification and regression tasks at all considered support set sizes. The trends of these mean ranks are consistent to the trends of the results in Figure 1.

**Statistical Comparison.** We perform two-sided Wilcoxon signed-rank tests [51] to compare the performance differences between ADKF and the next best method, namely, DKT. The null hypothesis is that the median of their performance differences on all FS-Mol test tasks is zero. Table 2 shows the  $p$ -values from this test, which indicates that the median of the performance differences is nonzero (i.e., ADKF significantly outperforms DKT) for the classification task at all considered support set sizes and for the regression task at support set sizes 64, 128, and 256 (at significance level  $\alpha = 0.05$ ).

**Ablation Study.** To show that 1) the bilevel optimization objective for ADKF is essential in learning adaptive feature representations and 2) the performance gains of ADKF do not just come from tuning the GP hyperparameters  $\theta$  at meta-test time, we consider two ablation models: DKT+ and ADKF-. The test performance of these models are shown in Figure 2. For ADKF-, we follow the ADKF training scheme but assume  $\partial \theta^* / \partial \phi = 0$ , i.e., the feature extractor parameters  $\phi$  are updated using the *direct gradient*  $\partial \mathcal{L}_V / \partial \phi$  rather than  $d \mathcal{L}_V / d \phi$ . The results show that ADKF- consistently underperforms ADKF, indicating that the total derivative for the bilevel optimization objective has non-negligible contributions to learning better feature representations. For DKT+, we take a model trained by DKT and adjust the GP hyperparameters  $\theta$  for each task at meta-test time. The results show that DKT+ has similar or worse performance compared to DKT, indicating that tuning the GP hyperparameters  $\theta$  at meta-test time is not sufficient for obtaining better test performance with DKT.



(a) Classification (157 tasks).



(b) Regression (111 tasks).

Figure 2: Mean performance with standard errors of DKT, ADKF, and two ablation models (DKT+ and ADKF-) on all FS-Mol test tasks. ADKF- is like ADKF but assuming  $\partial \theta^* / \partial \phi = 0$ , i.e., updating  $\phi$  with the direct gradient  $\partial \mathcal{L}_V / \partial \phi$ . DKT+ is like DKT but tuning the GP hyperparameters  $\theta$  during meta-testing.

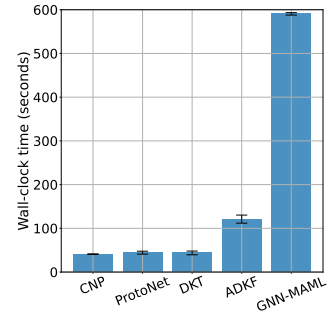


Figure 3: Wall-clock time consumed when meta-testing on a pre-defined set of FS-Mol tasks using each of the compared meta-learning methods.

Table 3: Mean performance with standard errors (broken down by EC category) of selected methods on all FS-Mol test tasks at support set size 64.

(a) Classification ( $\Delta$ AUPRC).

FS-Mol sub-benchmark (EC category)			Method				
Class	Description	#tasks	RF	GP-ST	ProtoNet	DKT	ADKF
1	oxidoreductases	7	$0.156 \pm 0.044$	$0.152 \pm 0.040$	$0.137 \pm 0.037$	$0.145 \pm 0.040$	<b><math>0.160 \pm 0.045</math></b>
2	kinases	125	$0.152 \pm 0.009$	$0.161 \pm 0.009$	$0.285 \pm 0.010$	$0.282 \pm 0.010$	<b><math>0.299 \pm 0.010</math></b>
3	hydrolases	20	$0.229 \pm 0.032$	$0.230 \pm 0.032$	$0.245 \pm 0.034$	$0.254 \pm 0.034$	<b><math>0.262 \pm 0.033</math></b>
4	lysases	2	$0.276 \pm 0.182$	<b><math>0.284 \pm 0.189</math></b>	$0.265 \pm 0.211$	$0.272 \pm 0.206$	$0.279 \pm 0.201$
5	isomerases	1	$0.166 \pm 0.040$	<b><math>0.212 \pm 0.052</math></b>	$0.172 \pm 0.044$	$0.204 \pm 0.058$	$0.198 \pm 0.046$
6	ligases	1	$0.149 \pm 0.035$	$0.199 \pm 0.028$	$0.170 \pm 0.028$	$0.229 \pm 0.013$	<b><math>0.231 \pm 0.022</math></b>
7	translocases	1	<b><math>0.128 \pm 0.039</math></b>	$0.109 \pm 0.049$	$0.099 \pm 0.028$	$0.122 \pm 0.022$	$0.109 \pm 0.033$
all enzymes			$0.163 \pm 0.009$	$0.171 \pm 0.009$	$0.271 \pm 0.009$	$0.271 \pm 0.010$	<b><math>0.285 \pm 0.010</math></b>

(b) Regression ( $R^2_{os}$ ).

FS-Mol sub-benchmark (EC category)			Method				
Class	Description	#tasks	RF	GP-ST	CNP	DKT	ADKF
1	oxidoreductases	6	$0.108 \pm 0.087$	$0.103 \pm 0.076$	$-0.012 \pm 0.011$	$0.098 \pm 0.078$	<b><math>0.116 \pm 0.079</math></b>
2	kinases	82	$0.160 \pm 0.019$	$0.162 \pm 0.022$	$0.127 \pm 0.017$	$0.343 \pm 0.022$	<b><math>0.363 \pm 0.024</math></b>
3	hydrolases	19	$0.256 \pm 0.058$	$0.267 \pm 0.061$	$0.014 \pm 0.015$	$0.295 \pm 0.063$	<b><math>0.310 \pm 0.062</math></b>
4	lysases	2	$0.418 \pm 0.405$	$0.417 \pm 0.416$	$0.100 \pm 0.068$	$0.440 \pm 0.418$	<b><math>0.442 \pm 0.403</math></b>
5	isomerases	1	$0.125 \pm 0.077$	$0.086 \pm 0.082$	$-0.012 \pm 0.010$	$0.209 \pm 0.113$	<b><math>0.226 \pm 0.063</math></b>
6	ligases	1	$0.182 \pm 0.040$	$0.202 \pm 0.079$	$0.002 \pm 0.004$	$0.277 \pm 0.035$	<b><math>0.279 \pm 0.043</math></b>
all enzymes			$0.178 \pm 0.019$	$0.181 \pm 0.021$	$0.097 \pm 0.014$	$0.321 \pm 0.021$	<b><math>0.340 \pm 0.022</math></b>

**Sub-benchmark Performance.** The test tasks in FS-Mol can be partitioned by Enzyme Commission (EC) number [49], which enables sub-benchmark evaluation within the entire benchmark. Ideally, the best method should be able to perform well across all sub-benchmarks. Table 3 shows the test performance of selected methods on all sub-benchmarks at support set size 64 (the median of all considered support sizes) for both the classification and regression tasks. The results indicate that, in addition to achieving best overall performance, ADKF has the best performance on all sub-benchmarks for the regression task and more than half sub-benchmarks for the classification task.

**Meta-testing Cost.** Figure 3 shows meta-testing costs of all compared meta-learning methods. ADKF is  $\sim 2.5$ x slower than CNP, ProtoNet, and DKT, but still much faster than GNN-MAML. We stress that this is not an important metric, as real-time adaptation is not required in this specific application.

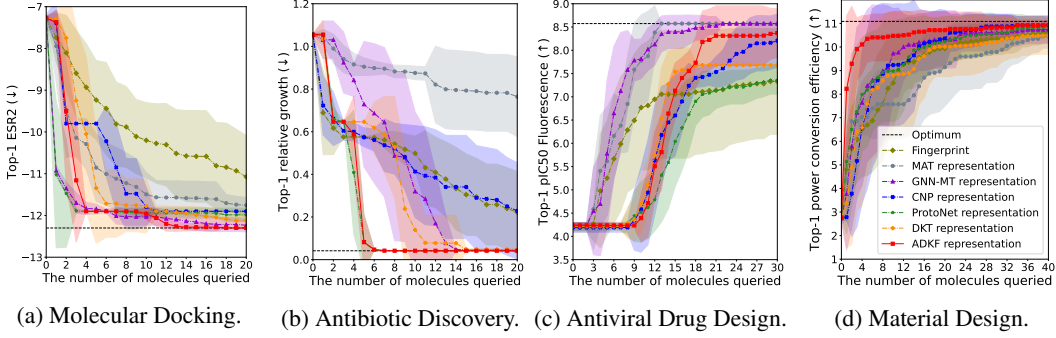


Figure 4: Mean top-1 target values with standard errors as a function of the number of molecules queried for all compared feature representations on four out-of-domain molecular optimization tasks.

## 5.2 Out-of-domain Molecular Optimization

We further show that the feature representation learned by ADKF is useful not only for in-domain molecular property prediction tasks but also for out-of-domain molecular optimization tasks. For this, we perform experiments involving finding molecules with best desired properties within given datasets using Bayesian optimization (BO) with GPs and the expected improvement acquisition function [17] with query-batch size 1. We use the Tanimoto kernel for fingerprint (with radius 2 and 2,048 bits based on count simulation) and Matérn52 kernel without ARD for all the other compared feature representations. All compared feature representations are extracted from the models trained on the FS-Mol dataset from scratch in Section 5.1, except for the pretrained MAT representation and fingerprint. We compare them on the following four representative molecular design tasks.

**a) Molecular Docking:** We create a dataset of 2,312 molecules sampled from the DockString [10] training set. The goal is to find molecules with best ESR2 binding scores within the dataset. The binding scores are calculated based on molecular docking using AutoDock Vina [46]. **b) Antibiotic Discovery:** We take a real-world dataset provided in [42] for developing antibiotics against *E. coli* BW25113, which contains 2,335 molecules. The goal is to find best molecules for growth inhibition against *E. coli* BW25113 within the dataset. **c) Antiviral Drug Design:** We take a real-world dataset provided in an open-source project, COVID Moonshot [5], for developing unpatented oral antiviral drug to treat SARS-CoV-2 (the virus causing COVID-19). The dataset contains 1,926 molecules with available IC50 Fluorescence measurement. The goal is to find molecules with top IC50 Fluorescence within the dataset. Since IC50 values span orders of magnitude, we instead maximize  $\text{pIC50}$  for the ease of modelling. **d) Material Design:** We create a dataset of 2,012 molecules sampled from the dataset provided in the Harvard Clean Energy Project [14]. The goal is to find organic molecules with top power conversion efficiency within the dataset. The photovoltaic efficiency is calculated based on expensive DFT simulations.

We repeat each experiment 20 times, each time starting from 16 randomly sampled molecules from the worst  $\sim 700$  molecules within the dataset. Results of these experiments are shown in Figure 4. It can be seen that the ADKF representation enables fastest discovery of top performing molecules for the molecular docking, antibiotic discovery, and material design tasks. For the antiviral drug discovery task, although the ADKF representation underperforms the MAT and GNN-MT representations, it still achieves competitive performance compared to other baselines.

## 6 Conclusion and Future Work

**Conclusion.** We have proposed Adaptive Deep Kernel Fitting (ADKF), a novel framework for deep kernel fitting that interpolates between meta-learning and conventional learning. ADKF meta-learns a feature extractor across tasks such that the task-specific GP models estimated on top of the extracted feature representations can achieve low prediction error on average across tasks. ADKF is implemented by solving a bilevel optimization objective via implicit differentiation. We have showed that ADKF learns generally useful feature representations, achieving state-of-the-art performance on real-world few-shot molecular prediction tasks and on out-of-domain molecular optimization tasks.

**Future Work.** Some directions for future work are as follows: 1) using ARD in the base kernel so that feature selection for each individual task can be done by the GP model, with potential overfitting problems being reduced by assuming a sparse prior over lengthscales or by learning a low-dimensional manifold for them; 2) adapting the feature extractor to each task as well by allowing small deviations across tasks according to a meta-learned prior on the feature extractor parameters (e.g., as described in [3]); 3) adopting a more principled approximate inference strategy for few-shot GP classification (e.g., using Pólya-Gamma data augmentation [39] or Laplace approximation [18]).

## Acknowledgments and Disclosure of Funding

We thank Massimiliano Patacchiola, John Bronskill, Marcin Sendera, and Richard E. Turner for helpful discussions and feedback. WC acknowledges funding via a Cambridge Trust Scholarship (supported by the Cambridge Trust) and a Cambridge University Engineering Department Studentship (under grant G105682 NMZR/089 supported by Huawei R&D UK). AT acknowledges funding via a C T Taylor Cambridge International Scholarship. JMHL acknowledges support from a Turing AI Fellowship under grant EP/V023756/1.

## References

- [1] Yoshua Bengio. Gradient-based optimization of hyperparameters. *Neural computation*, 12(8):1889–1900, 2000.
- [2] Da Chen, Yuefeng Chen, Yuhong Li, Feng Mao, Yuan He, and Hui Xue. Self-supervised learning for few-shot image classification. In *ICASSP 2021-2021 IEEE International Conference on Acoustics, Speech and Signal Processing (ICASSP)*, pages 1745–1749. IEEE, 2021.
- [3] Yutian Chen, Abram L Friesen, Feryal Behbahani, Arnaud Doucet, David Budden, Matthew Hoffman, and Nando de Freitas. Modular meta-learning with shrinkage. In H. Larochelle, M. Ranzato, R. Hadsell, M.F. Balcan, and H. Lin, editors, *Advances in Neural Information Processing Systems*, volume 33, pages 2858–2869. Curran Associates, Inc., 2020.
- [4] Ross M Clarke, Elre Talea Oldewage, and José Miguel Hernández-Lobato. Scalable one-pass optimisation of high-dimensional weight-update hyperparameters by implicit differentiation. In *International Conference on Learning Representations*, 2022.
- [5] The COVID Moonshot Consortium, Hagit Achdout, Anthony Aimon, Elad Bar-David, Haim Barr, Amir Ben-Shmuel, James Bennett, Vitaliy A. Bilenko, Vitaliy A. Bilenko, Melissa L. Boby, Bruce Borden, Gregory R. Bowman, Juliane Brun, Sarma BVNBS, Mark Calmiano, Anna Carbery, Daniel Carney, Emma Cattermole, Edcon Chang, Eugene Chernyshenko, John D. Chodera, Austin Clyde, Joseph E. Coffland, Galit Cohen, Jason Cole, Alessandro Contini, Lisa Cox, Milan Cvitkovic, Alex Dias, Kim Donckers, David L. Dotson, Alice Douangamath, Shirly Duberstein, Tim Dudgeon, Louise Dunnett, Peter K. Eastman, Noam Erez, Charles J. Eyermann, Mike Fairhead, Gwen Fate, Daren Fearon, Oleg Fedorov, Matteo Ferla, Rafaela S. Fernandes, Lori Ferrins, Richard Foster, Holly Foster, Ronen Gabizon, Adolfo Garcia-Sastre, Victor O. Gawriljuk, Paul Gehrtz, Carina Gileadi, Charline Giroud, William G. Glass, Robert Glen, Itai Glinert, Andre S. Godoy, Marian Gorichko, Tyler Gorrie-Stone, Ed J. Griffen, Storm Hassell Hart, Jag Heer, Michael Henry, Michelle Hill, Sam Horrell, Victor D. Huliak, Matthew F.D. Hurley, Tomer Israely, Andrew Jajack, Jitske Jansen, Eric Jnoff, Dirk Jochmans, Tobias John, Steven De Jonghe, Anastassia L. Kantsadi, Peter W. Kenny, J. L. Kiappes, Serhii O. Kinakh, Lizbe Koekemoer, Boris Kovar, Tobias Krojer, Alpha Lee, Bruce A. Lefker, Haim Levy, Ivan G. Logvinenko, Nir London, Petra Lukacik, Hannah Bruce Macdonald, Beth MacLean, Tika R. Malla, Tatiana Matviiuk, William McCorkindale, Briana L. McGovern, Sharon Melamed, Kostiantyn P. Melnykov, Oleg Michurin, Halina Mikolajek, Bruce F. Milne, Aaron Morris, Garrett M. Morris, Melody Jane Morwitzer, Demetri Moustakas, Aline M. Nakamura, Jose Brandao Neto, Johan Neyts, Luong Nguyen, Gabriela D. Noske, Vladas Oleinikovas, Glaucus Oliva, Gijs J. Overheul, David Owen, Ruby Pai, Jin Pan, Nir Paran, Benjamin Perry, Maneesh Pingle, Jakir Pinjari, Boaz Politi, Ailsa Powell, Vladimir Psenak, Reut Puni, Victor L. Rangel, Rambabu N. Reddi, St Patrick Reid, Efrat Resnick, Emily Grace Ripka, Matthew C. Robinson, Ralph P. Robinson, Jaime Rodriguez-Guerra, Romel Rosales, Dominic Rufa, Kadi Saar, Kumar Singh Saikatendu, Chris Schofield, Mikhail Shafeev, Aarif Shaikh, Jiye Shi, Khriesto Shurrush, Sukrit Singh, Assa Sittner, Rachael Skyner, Adam Smalley,

Bart Smeets, Mihaela D. Smilova, Leonardo J. Solmesky, John Spencer, Claire Strain-Damerell, Vishwanath Swamy, Hadas Tamir, Rachael Tennant, Warren Thompson, Andrew Thompson, Susana Tomasio, Igor S. Tsurupa, Anthony Tumber, Ioannis Vakonakis, Ronald P. van Rij, Laura Vangeel, Finny S. Varghese, Mariana Vaschetto, Einat B. Vitner, Vincent Voelz, Andrea Volkamer, Frank von Delft, Annette von Delft, Martin Walsh, Walter Ward, Charlie Weatherall, Shay Weiss, Kris M. White, Conor Francis Wild, Matthew Wittmann, Nathan Wright, Yfat Yahalom-Ronen, Daniel Zaidmann, Hadeer Zidane, and Nicole Zitzmann. Open science discovery of oral non-covalent sars-cov-2 main protease inhibitor therapeutics. *bioRxiv*, 2022.

[6] Gabriele Corso, Luca Cavalleri, Dominique Beaini, Pietro Liò, and Petar Veličković. Principal neighbourhood aggregation for graph nets. In H. Larochelle, M. Ranzato, R. Hadsell, M.F. Balcan, and H. Lin, editors, *Advances in Neural Information Processing Systems*, volume 33, pages 13260–13271. Curran Associates, Inc., 2020.

[7] Jia Deng, Wei Dong, Richard Socher, Li-Jia Li, Kai Li, and Li Fei-Fei. Imagenet: A large-scale hierarchical image database. In *2009 IEEE conference on computer vision and pattern recognition*, pages 248–255. Ieee, 2009.

[8] Chelsea Finn, Pieter Abbeel, and Sergey Levine. Model-agnostic meta-learning for fast adaptation of deep networks. In Doina Precup and Yee Whye Teh, editors, *Proceedings of the 34th International Conference on Machine Learning*, volume 70 of *Proceedings of Machine Learning Research*, pages 1126–1135. PMLR, 06–11 Aug 2017.

[9] Peter I Frazier. A tutorial on bayesian optimization. *arXiv preprint arXiv:1807.02811*, 2018.

[10] Miguel García-Ortegón, Gregor NC Simm, Austin J Tripp, José Miguel Hernández-Lobato, Andreas Bender, and Sergio Bacallado. Dockstring: easy molecular docking yields better benchmarks for ligand design. *arXiv preprint arXiv:2110.15486*, 2021.

[11] Marta Garnelo, Dan Rosenbaum, Christopher Maddison, Tiago Ramalho, David Saxton, Murray Shanahan, Yee Whye Teh, Danilo Rezende, and S. M. Ali Eslami. Conditional neural processes. In Jennifer Dy and Andreas Krause, editors, *Proceedings of the 35th International Conference on Machine Learning*, volume 80 of *Proceedings of Machine Learning Research*, pages 1704–1713. PMLR, 10–15 Jul 2018.

[12] Damien Garreau, Wittawat Jitkrittum, and Motonobu Kanagawa. Large sample analysis of the median heuristic. *arXiv preprint arXiv:1707.07269*, 2017.

[13] Justin Gilmer, Samuel S. Schoenholz, Patrick F. Riley, Oriol Vinyals, and George E. Dahl. Neural message passing for quantum chemistry. In Doina Precup and Yee Whye Teh, editors, *Proceedings of the 34th International Conference on Machine Learning*, volume 70 of *Proceedings of Machine Learning Research*, pages 1263–1272. PMLR, 06–11 Aug 2017.

[14] Johannes Hachmann, Roberto Olivares-Amaya, Sule Atahan-Evrenk, Carlos Amador-Bedolla, Roel S Sánchez-Carrera, Aryeh Gold-Parker, Leslie Vogt, Anna M Brockway, and Alán Aspuru-Guzik. The harvard clean energy project: large-scale computational screening and design of organic photovoltaics on the world community grid. *The Journal of Physical Chemistry Letters*, 2(17):2241–2251, 2011.

[15] Geoffrey E Hinton and Russ R Salakhutdinov. Using deep belief nets to learn covariance kernels for gaussian processes. In J. Platt, D. Koller, Y. Singer, and S. Roweis, editors, *Advances in Neural Information Processing Systems*, volume 20. Curran Associates, Inc., 2007.

[16] Yuqing Hu, Vincent Gripon, and Stéphane Pateux. Leveraging the feature distribution in transfer-based few-shot learning. In *International Conference on Artificial Neural Networks*, pages 487–499. Springer, 2021.

[17] Donald R Jones, Matthias Schonlau, and William J Welch. Efficient global optimization of expensive black-box functions. *Journal of Global optimization*, 13(4):455–492, 1998.

[18] Minyoung Kim and Timothy Hospedales. Gaussian process meta few-shot classifier learning via linear discriminant laplace approximation. *arXiv preprint arXiv:2111.05392*, 2021.

[19] Diederik P Kingma and Jimmy Ba. Adam: A method for stochastic optimization. *arXiv preprint arXiv:1412.6980*, 2014.

[20] Brenden Lake, Ruslan Salakhutdinov, Jason Gross, and Joshua Tenenbaum. One shot learning of simple visual concepts. In *Proceedings of the annual meeting of the cognitive science society*, volume 33, 2011.

[21] J. Larsen, L.K. Hansen, C. Svarer, and M. Ohlsson. Design and regularization of neural networks: the optimal use of a validation set. In *Neural Networks for Signal Processing VI. Proceedings of the 1996 IEEE Signal Processing Society Workshop*, pages 62–71, 1996.

[22] Kwonjoon Lee, Subhransu Maji, Avinash Ravichandran, and Stefano Soatto. Meta-learning with differentiable convex optimization. In *Proceedings of the IEEE/CVF Conference on Computer Vision and Pattern Recognition (CVPR)*, June 2019.

[23] Dong C Liu and Jorge Nocedal. On the limited memory bfgs method for large scale optimization. *Mathematical programming*, 45(1):503–528, 1989.

[24] Jonathan Lorraine, Paul Vicol, and David Duvenaud. Optimizing millions of hyperparameters by implicit differentiation. In Silvia Chiappa and Roberto Calandra, editors, *Proceedings of the Twenty Third International Conference on Artificial Intelligence and Statistics*, volume 108 of *Proceedings of Machine Learning Research*, pages 1540–1552. PMLR, 26–28 Aug 2020.

[25] Jelena Luketina, Mathias Berglund, Klaus Greff, and Tapani Raiko. Scalable gradient-based tuning of continuous regularization hyperparameters. In Maria Florina Balcan and Kilian Q. Weinberger, editors, *Proceedings of The 33rd International Conference on Machine Learning*, volume 48 of *Proceedings of Machine Learning Research*, pages 2952–2960, New York, New York, USA, 20–22 Jun 2016. PMLR.

[26] Łukasz Maziarka, Tomasz Danel, Sławomir Mucha, Krzysztof Rataj, Jacek Tabor, and Stanisław Jastrzębski. Molecule attention transformer. *arXiv preprint arXiv:2002.08264*, 2020.

[27] David Mendez, Anna Gaulton, A Patrícia Bento, Jon Chambers, Marleen De Veij, Eloy Félix, María Paula Magariños, Juan F Mosquera, Prudence Mutowo, Michał Nowotka, et al. Chemb3l: towards direct deposition of bioassay data. *Nucleic acids research*, 47(D1):D930–D940, 2019.

[28] Radford M Neal. *Bayesian Learning for Neural Networks*. PhD thesis, University of Toronto, 1996.

[29] Sebastian W. Ober, Carl E. Rasmussen, and Mark van der Wilk. The promises and pitfalls of deep kernel learning. In Cassio de Campos and Marloes H. Maathuis, editors, *Proceedings of the Thirty-Seventh Conference on Uncertainty in Artificial Intelligence*, volume 161 of *Proceedings of Machine Learning Research*, pages 1206–1216. PMLR, 27–30 Jul 2021.

[30] Eunbyung Park and Junier B Oliva. Meta-curvature. In H. Wallach, H. Larochelle, A. Beygelzimer, F. d’Alché-Buc, E. Fox, and R. Garnett, editors, *Advances in Neural Information Processing Systems*, volume 32. Curran Associates, Inc., 2019.

[31] Massimiliano Patacchiola, Jack Turner, Elliot J. Crowley, Michael O’Boyle, and Amos J Storkey. Bayesian meta-learning for the few-shot setting via deep kernels. In H. Larochelle, M. Ranzato, R. Hadsell, M. F. Balcan, and H. Lin, editors, *Advances in Neural Information Processing Systems*, volume 33, pages 16108–16118. Curran Associates, Inc., 2020.

[32] Fabian Pedregosa. Hyperparameter optimization with approximate gradient. In Maria Florina Balcan and Kilian Q. Weinberger, editors, *Proceedings of The 33rd International Conference on Machine Learning*, volume 48 of *Proceedings of Machine Learning Research*, pages 737–746, New York, New York, USA, 20–22 Jun 2016. PMLR.

[33] Lutz Prechelt. Early stopping-but when? In *Neural Networks: Tricks of the trade*, pages 55–69. Springer, 1998.

[34] Aravind Rajeswaran, Chelsea Finn, Sham M Kakade, and Sergey Levine. Meta-learning with implicit gradients. In H. Wallach, H. Larochelle, A. Beygelzimer, F. d’Alché-Buc, E. Fox, and R. Garnett, editors, *Advances in Neural Information Processing Systems*, volume 32. Curran Associates, Inc., 2019.

[35] Liva Ralaivola, Sanjay J Swamidass, Hiroto Saigo, and Pierre Baldi. Graph kernels for chemical informatics. *Neural networks*, 18(8):1093–1110, 2005.

[36] Carl Edward Rasmussen and Christopher K. I. Williams. *Gaussian Processes for Machine Learning*. Adaptive Computation and Machine Learning. MIT Press, Cambridge, MA, USA, January 2006.

[37] David Rogers and Mathew Hahn. Extended-connectivity fingerprints. *Journal of chemical information and modeling*, 50(5):742–754, 2010.

[38] Jake Snell, Kevin Swersky, and Richard Zemel. Prototypical networks for few-shot learning. In I. Guyon, U. V. Luxburg, S. Bengio, H. Wallach, R. Fergus, S. Vishwanathan, and R. Garnett, editors, *Advances in Neural Information Processing Systems*, volume 30. Curran Associates, Inc., 2017.

[39] Jake Snell and Richard Zemel. Bayesian few-shot classification with one-vs-each pólya-gamma augmented gaussian processes. *arXiv preprint arXiv:2007.10417*, 2020.

[40] Megan Stanley, John F Bronskill, Krzysztof Maziarz, Hubert Misztela, Jessica Lanini, Marwin Segler, Nadine Schneider, and Marc Brockschmidt. Fs-mol: A few-shot learning dataset of molecules. In *Thirty-fifth Conference on Neural Information Processing Systems Datasets and Benchmarks Track (Round 2)*, 2021.

[41] Teague Sterling and John J Irwin. Zinc 15-ligand discovery for everyone. *Journal of chemical information and modeling*, 55(11):2324–2337, 2015.

[42] Jonathan M. Stokes, Kevin Yang, Kyle Swanson, Wengong Jin, Andres Cubillos-Ruiz, Nina M. Donghia, Craig R. MacNair, Shawn French, Lindsey A. Carfrae, Zohar Bloom-Ackermann, Victoria M. Tran, Anush Chiappino-Pepe, Ahmed H. Badran, Ian W. Andrews, Emma J. Chory, George M. Church, Eric D. Brown, Tommi S. Jaakkola, Regina Barzilay, and James J. Collins. A deep learning approach to antibiotic discovery. *Cell*, 180(4):688–702.e13, 2020.

[43] Yonglong Tian, Yue Wang, Dilip Krishnan, Joshua B Tenenbaum, and Phillip Isola. Rethinking few-shot image classification: a good embedding is all you need? In *European Conference on Computer Vision*, pages 266–282. Springer, 2020.

[44] Prudencio Tossou, Basile Dura, Francois Laviolette, Mario Marchand, and Alexandre Lacoste. Adaptive deep kernel learning. *arXiv preprint arXiv:1905.12131*, 2019.

[45] Eleni Triantafillou, Tyler Zhu, Vincent Dumoulin, Pascal Lamblin, Utku Evci, Kelvin Xu, Ross Goroshin, Carles Gelada, Kevin Swersky, Pierre-Antoine Manzagol, et al. Meta-dataset: A dataset of datasets for learning to learn from few examples. *arXiv preprint arXiv:1903.03096*, 2019.

[46] Oleg Trott and Arthur J Olson. Autodock vina: improving the speed and accuracy of docking with a new scoring function, efficient optimization, and multithreading. *Journal of computational chemistry*, 31(2):455–461, 2010.

[47] Oriol Vinyals, Charles Blundell, Timothy Lillicrap, koray kavukcuoglu, and Daan Wierstra. Matching networks for one shot learning. In D. Lee, M. Sugiyama, U. Luxburg, I. Guyon, and R. Garnett, editors, *Advances in Neural Information Processing Systems*, volume 29. Curran Associates, Inc., 2016.

[48] Yuanhao Wang\*, Guodong Zhang\*, and Jimmy Ba. On solving minimax optimization locally: A follow-the-ridge approach. In *International Conference on Learning Representations*, 2020.

[49] Oren F. Webb, Tommy J. Phelps, Paul R. Bienkowski, Philip M. Digrazia, David C. White, and Gary S. Sayler. Enzyme nomenclature, 1992.

[50] Florian Wenzel, Théo Galy-Fajou, Christian Donner, Marius Kloft, and Manfred Opper. Efficient gaussian process classification using pólya-gamma data augmentation. In *Proceedings of the AAAI Conference on Artificial Intelligence*, volume 33, pages 5417–5424, 2019.

[51] Frank Wilcoxon. Individual comparisons by ranking methods. In *Breakthroughs in statistics*, pages 196–202. Springer, 1992.

[52] Andrew Gordon Wilson, Zhitong Hu, Ruslan Salakhutdinov, and Eric P. Xing. Deep kernel learning. In Arthur Gretton and Christian C. Robert, editors, *Proceedings of the 19th International Conference on Artificial Intelligence and Statistics*, volume 51 of *Proceedings of Machine Learning Research*, pages 370–378, Cadiz, Spain, 09–11 May 2016. PMLR.

## A Cauchy’s Implicit Function Theorem

We state Cauchy’s Implicit Function Theorem (IFT) in the context of ADKF in Theorem 1.

**Theorem 1 (Implicit Function Theorem (IFT))** *Let  $\mathcal{T}'$  be any given task. Suppose for some  $\psi'_{meta}$  and  $\psi'_{adapt}$  that  $\frac{\partial \mathcal{L}_T(\psi_{meta}, \psi_{adapt}, \mathcal{S}_{\mathcal{T}'})}{\partial \psi_{adapt}} \Big|_{\psi'_{meta}, \psi'_{adapt}} = \mathbf{0}$ . Suppose that  $\frac{\partial \mathcal{L}_T}{\partial \psi_{adapt}}(\psi_{meta}, \psi_{adapt}, \mathcal{T}') : \Psi_{meta} \times \Psi_{adapt} \rightarrow \Psi_{adapt}$  is a continuously differentiable function w.r.t.  $\psi_{meta}$  and  $\psi_{adapt}$  and the Hessian  $\frac{\partial^2 \mathcal{L}_T(\psi_{meta}, \psi_{adapt}, \mathcal{S}_{\mathcal{T}'})}{\partial \psi_{adapt} \partial \psi_{adapt}^T} \Big|_{\psi'_{meta}, \psi'_{adapt}}$  is invertible. Then, there exists an open set  $U \in \Psi_{meta}$  containing  $\psi'_{meta}$  and a function  $\psi_{adapt}^*(\psi_{meta}, \mathcal{S}_{\mathcal{T}'}) : \Psi_{meta} \rightarrow \Psi_{adapt}$ , such that  $\psi'_{adapt} = \psi_{adapt}^*(\psi'_{meta}, \mathcal{S}_{\mathcal{T}'})$  and  $\frac{\partial \mathcal{L}_T(\psi_{meta}, \psi_{adapt}, \mathcal{S}_{\mathcal{T}'})}{\partial \psi_{adapt}} \Big|_{\psi''_{meta}, \psi_{adapt}^*(\psi''_{meta}, \mathcal{S}_{\mathcal{T}'})} = \mathbf{0}$ ,  $\forall \psi''_{meta} \in U$ . Moreover, the rate at which  $\psi_{adapt}^*(\psi_{meta}, \mathcal{S}_{\mathcal{T}'})$  is changing w.r.t.  $\psi_{meta}$  for any  $\psi''_{meta} \in U$  is given by*

$$\begin{aligned} & \frac{\partial \psi_{adapt}^*(\psi_{meta}, \mathcal{S}_{\mathcal{T}'})}{\partial \psi_{meta}} \Big|_{\psi''_{meta}} \\ &= - \left( \frac{\partial^2 \mathcal{L}_T(\psi_{meta}, \psi_{adapt}, \mathcal{S}_{\mathcal{T}'})}{\partial \psi_{adapt} \partial \psi_{adapt}^T} \right)^{-1} \frac{\partial^2 \mathcal{L}_T(\psi_{meta}, \psi_{adapt}, \mathcal{S}_{\mathcal{T}'})}{\partial \psi_{adapt} \partial \psi_{meta}^T} \Big|_{\psi''_{meta}, \psi_{adapt}^*(\psi''_{meta}, \mathcal{S}_{\mathcal{T}'})}. \end{aligned}$$

## B Detailed Configurations of All Compared Methods

**Single-task Methods.** Single-task methods (RF, kNN, GP-ST, and GNN-ST) are trained on the support set of each test task, without leveraging the knowledge contained in the training tasks. The implementations of RF, kNN, and GNN-ST are taken from [40]. RF, kNN, and GP-ST operates on top of manually curated features obtained using RDKit. RF and kNN use extended connectivity fingerprint [37] (count-based fingerprint with radius 2 and size 2,048) and phys-chem descriptors (with size 42). GP-ST uses fingerprint (with radius 2 and 2,048 bits based on count simulation). Hyperparameter search configurations for these methods are based on the extensive industrial experience from the authors of [40]. GNN-ST uses a 8-layer GNN with a hidden dimension of 128 and a gated readout function [13], considering  $\sim 30$  hyperparameter search configurations.

**Multi-task Pretraining.** The implementation of GNN-MT is taken from [40]. GNN-MT shares a 10-layer GNN with a hidden dimension of 128 using principal neighborhood message aggregation [6] across tasks, and uses a task-specific gated readout function [13] and an MLP with one hidden layer on top for each individual task. The model is trained on the support sets of all training tasks with early stopping based on the validation performance on the validation tasks. The task-specific components of the model are fine-tuned for each test task.

**Self-supervised Pretraining.** The implementation of MAT is taken from [40]. We use the official pretrained model parameters [26], which is pretrained on 2 millions molecules sampled from the ZINC15 dataset [41]. We fine-tuned it for each test task with hyperparameter search and early stopping based on 20% of the support set associated with the task.

**Meta-learning Methods.** Meta-learning methods (ProtoNet, GNN-MAML, CNP, DKT, and ADKF) are designed for few-shot learning problems, which enables quick adaptation on unseen test tasks given a few labeled examples. The implementations of ProtoNet and GNN-MAML are taken from [40]. The GNN feature extractor used for GNN-MAML is the same as that used for GNN-ST. ProtoNet, CNP, DKT, and ADKF operates on top of a combination of extended connectivity fingerprint [37] (count-based fingerprint with radius 2 and size 2,048) and features extracted by a GNN. The feature extractor architecture used for CNP, DKT, and ADKF is the same as that used for ProtoNet in [40], with the size of the final feature representation being tuned on the validation tasks.

## C Further Experimental Results

Figures 5 and 6 show the box plots for the classification and regression performances of all compared methods on all FS-Mol test tasks, respectively.

## D Task-level Evaluation Metrics

**Binary Classification.** Following [40], the task-level metric used for the binary classification task in FS-Mol is the relative area under the precision-recall curve ( $\Delta\text{AUPRC}$ ), which is sensitive to the balance of the two classes in the query sets and allows for a comparison to the performance of a random classifier:

$$\begin{aligned}\Delta\text{AUPRC}(\text{target classifier } g, \mathcal{T}) &= \text{AUPRC}(\text{target classifier } g, \mathcal{Q}_\mathcal{T}) - \text{AUPRC}(\text{random classifier}, \mathcal{Q}_\mathcal{T}) \\ &= \text{AUPRC}(\text{target classifier } g, \mathcal{Q}_\mathcal{T}) - \frac{\#\text{positive data points in } \mathcal{Q}_\mathcal{T}}{N_{\mathcal{Q}_\mathcal{T}}}.\end{aligned}$$

**Regression.** We propose to use the out-of-sample coefficient of determination ( $R_{os}^2$ ) as the task-level metric for the regression task in FS-Mol, which takes into account forecast errors:

$$R_{os}^2(\text{target regressor } g, \mathcal{T}) = 1 - \frac{\sum_{(\mathbf{x}_m, y_m) \in \mathcal{Q}_\mathcal{T}} (y_m - g(\mathbf{x}_m))^2}{\sum_{y_m \in \mathcal{Q}_\mathcal{T}^y} (y_m - \bar{y}_{\mathcal{S}_\mathcal{T}})^2},$$

where  $\bar{y}_{\mathcal{S}_\mathcal{T}} = \frac{1}{N_{\mathcal{S}_\mathcal{T}}} \sum_{y_n \in \mathcal{S}_\mathcal{T}^y} y_n$  is the mean target value in the support set  $\mathcal{S}_\mathcal{T}$ . This is different from the regular coefficient of determination ( $R^2$ ), wherein the total sum of squares in the denominator are computed using the mean target value  $\bar{y}_{\mathcal{Q}_\mathcal{T}} = \frac{1}{N_{\mathcal{Q}_\mathcal{T}}} \sum_{y_m \in \mathcal{Q}_\mathcal{T}^y} y_m$  in the query set  $\mathcal{Q}_\mathcal{T}$ .

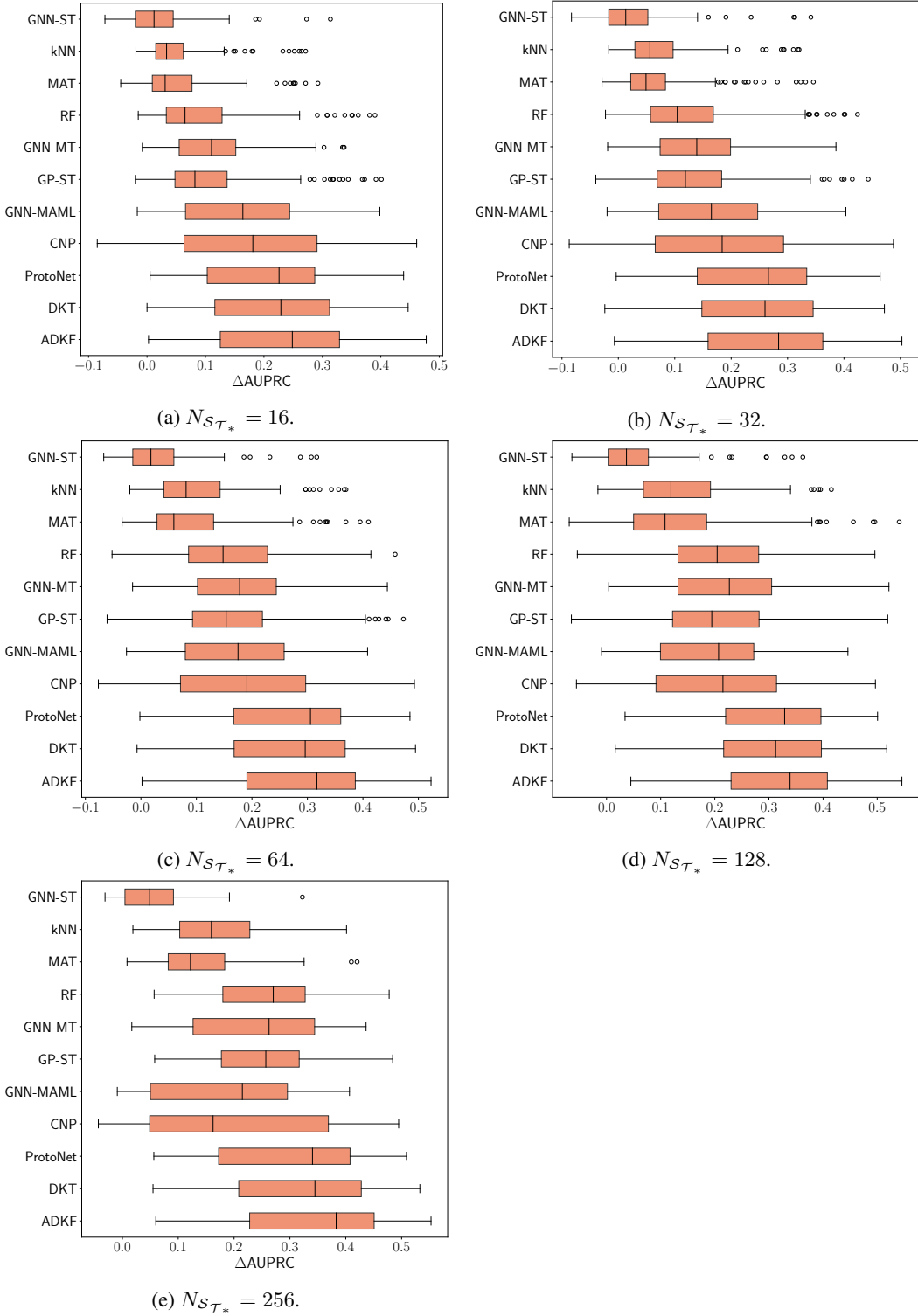


Figure 5: Box plots for the classification performance of all compared methods on 157 FS-Mol test tasks at different support set sizes.

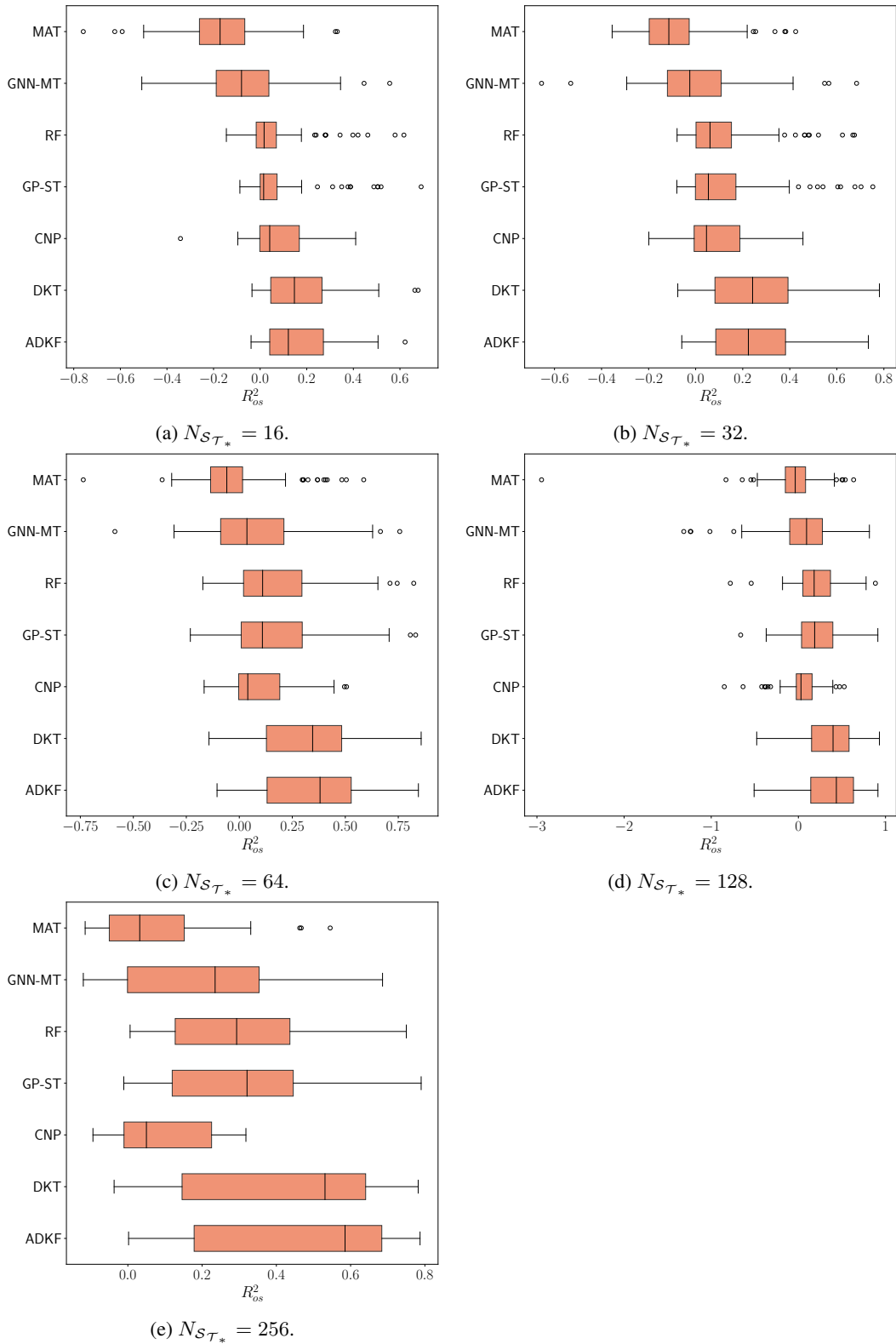


Figure 6: Box plots for the regression performance of all compared methods on 111 FS-Mol test tasks at different support set sizes.